Magnetic helicity analysis of an interplanetary twisted flux tube

Sergio Dasso, Cristina H. Mandrini, Pascal Démoulin, Charles J. Farrugia

JOURNAL OF GEOPHYSICAL RESEARCH, VOL. 108, NO. A10, 1362, doi:10.1029/2003JA009942, 2003

Magnetic helicity analysis of an interplanetary twisted flux tube

S. Dasso and C. H. Mandrini
Instituto de Astronomía y Física del Espacio (IAFE), Buenos Aires, Argentina

P. Démoulin
Observatoire de Paris, LESIA, Meudon, France

C. J. Farrugia
Institute for the Study of Earth, Oceans, and Space, University of New Hampshire, Durham, New Hampshire, USA

Received 17 March 2003; revised 26 June 2003; accepted 3 July 2003; published 14 October 2003.

[1] We compute the magnetic flux and helicity of an interplanetary flux tube observed by the spacecraft Wind on 24–25 October 1995. We investigate how model-dependent are the results by determining the flux-tube orientation using two different methods (minimum variance and a simultaneous fit), and three different models: a linear force-free field, a uniformly twisted field, and a nonforce-free field with constant current. We have fitted the set of free parameters for the six cases and have found that the two force-free models fit the data with very similar quality for both methods. Then, both the comparable computed parameters and global quantities, magnetic flux and helicity per unit length, agree to within 10% for the two force-free models. These results imply that the magnetic flux and helicity of the tube are well-determined quantities, nearly independent of the model used, provided that the fit to the data is good enough. *INDEX TERMS:* 2111 Interplanetary Physics: Ejecta, driver gases, and magnetic clouds; 2134 Interplanetary Physics: Interplanetary magnetic fields; 7524 Solar Physics, Astrophysics, and Astronomy: Magnetic fields; 7513 Solar Physics, Astrophysics, and Astronomy: Coronal mass ejections; 7827 Space Plasma Physics: Kinetic and MHD theory; *KEYWORDS:* interplanetary physics, solar wind, magnetic flux ropes, interplanetary coronal mass ejections, magnetic helicity

Citation: Dasso, S., C. Mandrini, P. Démoulin, and C. J. Farrugia, Magnetic helicity analysis of an interplanetary twisted flux tube, *J. Geophys. Res.*, *108*(A10), 1362, doi:10.1029/2003JA009942, 2003.

1. Introduction

[2] Solar ejecta are transient structures that perturb the solar wind as they move away from the Sun. When expelled toward the Earth, depending of their orientation and their magnetic helicity, these objects can trigger significant geomagnetic perturbations as a consequence of reconnection processes in the terrestrial magnetopause [see, e.g., *Farrugia et al.*, 1997; *Gonzalez et al.*, 1999, and references therein].

[3] In situ observations show that the proton temperature (T_p) in interplanetary flux tubes is frequently lower than in the solar wind [see, e.g., *Gosling*, 1990; *Richardson and Cane*, 1995, and references therein]. However, the electron temperature, T_e, is frequently higher than the proton temperature [*Osherovich et al.*, 1993; *Richardson et al.*, 1997], and so the electron pressure can play a significant role in their dynamical magnetic configuration. Interplanetary magnetic clouds (MCs) form an important subset of solar ejecta, which are characterized by enhanced magnetic field strength with respect to ambient values, a large rotation of the magnetic field vector, and low T_p [*Burlaga et al.*, 1981; *Burlaga*, 1995]. Although the mean value of the plasma beta of protons, $\beta_p = 8\pi n_p k_B T_p/B^2$ (where n_p is the proton density, B is the magnetic field intensity, and k_B is the Boltzmann's constant), in MCs is frequently low (typically $\beta_p \sim 0.1$), values of $\beta_p \sim 0.2$–0.4 or even higher [see, e.g., *Dasso et al.*, 2001] have been observed.

[4] Magnetic helicity characterizes how magnetic field lines are twisted around each other [see, e.g., *Berger and Field*, 1984]. It plays a very important role in the frame of MHD theory because it is almost conserved, even in resistive MHD, on time scales shorter than the global diffusion time scale [*Berger*, 1984]. Magnetic helicity is observed in the solar wind on all scales, from more than 1 AU to less than the gyroradius of a thermal proton [*Smith*, 2000]. In a dynamically turbulent medium such as the solar wind, magnetic helicity tends to be transported to larger scales and to be condensed in the longest wavelength mode [see, e.g. *Matthaeus*, 2000]. In spite of its relevance, the magnetic helicity contained in solar ejecta, such as interplanetary flux tubes, is poorly known.

[5] Solar ejecta transport magnetic helicity from the Sun into the interplanetary medium. There is observational

0148-0227/03/2003JA009942

evidence showing that the helicity sign in magnetic clouds matches that of their source regions [see, e.g., *Bothmer and Schwenn*, 1994; *Rust*, 1994; *Marubashi*, 1997; *Yurchyshyn et al.*, 2001]. However, in a recent study, *Leamon et al.* [2002] found that the helicity sign of both objects, MCs and their source, agrees in only 62% of the analyzed cases and that the link can be solar cycle dependent. In the absence of any theoretical interpretation, this lower percentage, when compared with the aforementioned papers, could simply mean that we need a more accurate determination of the helicity in both MCs and in the corona using, at least, one magnetic model to fit the available data (since in both cases the data provide only partial information on the magnetic configuration). For example, a significant fraction of coronal sigmoids are observed as such because of projection effects or magnetic complexity [e.g., *Glover et al.*, 2000] (see also *Fletcher et al.* [2001] for a well-studied case); then, the shape of these sigmoids does not contain enough information on the helicity sign. In the interplanetary space, a magnetic model is also needed to accurately recover the global magnetic field structure from one dimensional data. One purpose of the present paper is to compare various approaches that have been proposed for the magnetic configuration.

[6] Interplanetary flux tubes or flux ropes, in particular MCs, frequently present a helical structure and can be modeled in a cylindrical geometry [*Farrugia et al.*, 1995] using different approaches: a linear force-free field [e.g., *Burlaga et al.*, 1981; *Burlaga*, 1988; *Lepping et al.*, 1990], a force-free uniformly twisted field [e.g., *Farrugia et al.*, 1999] or, supported on the possibility of an active role of the plasma pressure, even a nonforce-free model. In particular, several nonforce-free models have been recently applied to interplanetary flux tubes; for instance, in situ observations have been compared to: (1) two axially symmetric models, one with a constant current density [*Hidalgo et al.*, 2002] and another with an azimuthal current density depending linearly on the distance to the axis of the tube [*Cid et al.*, 2002], (2) a nonaxially symmetric model [*Hu and Sonnerup*, 2001], and (3) both cylindrically and noncylindrically symmetric models [*Mulligan and Russell*, 2001]. All these models are physically different, and it is not yet evident which of them give the best representation of interplanetary flux tubes. Authors usually use a given model and method consistently, but a comparison between the predictions of these various approaches has not yet been done.

[7] We analyze here the magnetic configuration of a flux tube observed by Wind on 24–25 October 1995 [*Farrugia et al.*, 1999, Figure 1]. Preliminary studies of the plasma and magnetic properties of this flux tube have been done by *Farrugia et al.* [1999] and *Dasso et al.* [2003a]. This flux tube presents a large and smooth rotation of the field and a low value of the proton plasma beta ($\beta_p \sim 0.2$–0.4), similar to what can be observed in MCs. However, near the center of the tube (around at 50% of its size) T_p was a factor $\sim$10 higher than at regions near its boundaries, and thus it is not classified as a MC but rather as a "hot flux tube." However, the value of β_p remains low because the higher temperature region has a lower density. The total β (including the contribution of electron and alpha particles to the pressure) is in the range of 0.8–1.0 for the entire event.

[8] In this work, we first (section 2) introduce the magnetic helicity expression for cylindrically symmetric structures, and in section 3 we derive the analytical expressions of the magnetic helicity for three models. Then, we apply these expressions (section 4) to this hot flux tube by fitting the set of free parameters (for each of the three models) to the magnetic field data. In each model, the orientation of the tube is computed using two different methods: first, a minimum variance (MV) analysis, and second, a simultaneous fit (SF) of all the parameters. We examine which model best represents the observations, and how model and method dependent the fitted parameters are. We then estimate global physical properties of the flux rope, specifically, its magnetic flux and helicity. In section 5 we give our conclusions.

2. Magnetic Helicity of Flux Tubes

[9] The magnetic helicity (H) of a field $\vec{\mathbf{B}}$ within a volume V is defined by $H = \int_V \vec{\mathbf{A}} \cdot \vec{\mathbf{B}}\, dV$, where the vector potential $\vec{\mathbf{A}}$ satisfies $\vec{\mathbf{B}} = \vec{\nabla} \times \vec{\mathbf{A}}$. However, the helicity as defined above is physically meaningful only when the magnetic field is fully contained inside the volume V (i.e., at any point of the surface S surrounding V, the normal component $B_N = \vec{\mathbf{B}} \cdot \hat{\mathbf{n}}$ vanishes). This is so because the vector potential is defined only up to a gauge transformation ($\vec{\mathbf{A}}' = \vec{\mathbf{A}} + \vec{\nabla}\Phi$), then H is gauge-invariant only when $B_n = 0$. For cases where $B_n \neq 0$ (as can happen on both "legs" of interplanetary flux tubes), it has been shown that a relative magnetic helicity (H_r) can be defined [*Berger and Field*, 1984]. This relative helicity is obtained by subtracting the helicity of a reference field $\vec{\mathbf{B}}_{\rm ref}$ having the same distribution of B_n on S:

$$H_r = H - \int_V \vec{\mathbf{A}}_{\rm ref} \cdot \vec{\mathbf{B}}_{\rm ref}\, dV. \tag{1}$$

H_r is gauge-invariant and does not depend on the common extension of $\vec{\mathbf{B}}$ and $\vec{\mathbf{B}}_{\rm ref}$ outside V, if $\vec{A} \times \hat{n} = \vec{A}_{\rm ref} \times \hat{n}$ on the surface S of V, as was shown by *Berger and Field* [1984].

[10] The magnetic field of an interplanetary flux tube can be modeled locally as a straight cylindrical structure with a two-component magnetic field $\vec{\mathbf{B}}(\vec{\mathbf{r}}) = B_\varphi(r)\hat{\varphi} + B_z(r)\hat{z}$. The reference field can be chosen as $\vec{\mathbf{B}}_{\rm ref}(r) = B_z(r)\hat{z}$ (with null magnetic helicity, since field lines are straight). Using the condition $\vec{A} \times \hat{n} = \vec{A}_{\rm ref} \times \hat{n}$ at the cylinder surface, H_r per unit length (L) can be expressed independently of $\vec{\mathbf{A}}_{\rm ref}$ and $\vec{\mathbf{B}}_{\rm ref}$ as,

$$H_r/L = 4\pi \int_0^R A_\varphi B_\varphi\, r dr, \tag{2}$$

where R is the radius of the tube.

3. Three Models

3.1. Linear Force-Free Field

[11] The general static, axially symmetric magnetic field of a linear force-free configuration ($\vec{\nabla} \times \vec{\mathbf{B}} = \alpha\vec{\mathbf{B}}$, with α constant) was obtained by *Lundquist* [1950]. However, it has been shown that one harmonic of this solution is enough to describe in situ measurements of interplanetary magnetic

flux tubes at 1 AU [e.g., *Burlaga et al.*, 1981; *Burlaga*, 1988; *Lepping et al.*, 1990]. Thus, the field is well modeled by

$$\vec{\mathbf{B}} = B_0 J_1(\alpha r)\hat{\varphi} + B_0 J_0(\alpha r)\hat{z}, \quad (3)$$

where J_n is the Bessel function of the first kind of order n, B_0 is the strength of the field and α is a constant. The magnetic field lines twist per unit length, $\tau = d\varphi/dz = B_\varphi/(rB_z)$, is:

$$\tau(r) = \frac{J_1(\alpha r)}{rJ_0(\alpha r)}. \quad (4)$$

[12] The constant α determines the twist at the flux tube axis, $\tau_0 = \tau(0) = \alpha/2$. The two physical parameters fitted are α and B_0. It is worth noting that we do not force B_z to vanish at the cloud border (as it was done in some previous analysis [e.g., *Lepping et al.*, 1990]). This allows us to have the same number of free parameters as in the next two models, turning the comparisons among them more straightforward.

[13] We obtain the relative helicity for this force-free field from equation (2), taking $\vec{\mathbf{A}} = \vec{\mathbf{B}}/\alpha$:

$$\frac{H_r}{L} = \frac{4\pi B_0^2}{\alpha}\int_0^R J_1^2(\alpha r) r dr = \left(\frac{8\pi}{U^4}\int_0^U J_1^2(u)\, u du\right) B_0^2 R^4 \tau_0, \quad (5)$$

where $u = 2\tau_0 r$ and $U = 2\tau_0 R$ are dimensionless quantities. In the last expression of equation (5), we have rewritten H_r/L to emphasize that it has the units of the magnetic flux to the second power ($(B_0R^2)^2$) multiplied by a twist per unit length (τ_0).

3.2. Uniformly Twisted Field

[14] The nonlinear force-free field with a uniform twist has been used to model interplanetary flux tubes [e.g., *Farrugia et al.*, 1999]. For this configuration, $\vec{\mathbf{B}}$ is given by [*Gold and Hoyle*, 1960],

$$\vec{\mathbf{B}} = \frac{B_0 br}{1 + b^2 r^2}\hat{\varphi} + \frac{B_0}{1 + b^2 r^2}\hat{z}. \quad (6)$$

In this magnetic configuration, the amount by which a given line is twisted is independent of r:

$$\tau(r) = \tau_0 = b. \quad (7)$$

The two physical parameters fitted are b and B_0.

[15] From equation (2) and

$$\vec{\mathbf{A}} = \frac{B_0}{2b^2 r}\ln\left(1 + b^2 r^2\right)\hat{\varphi} - \frac{B_0}{2b}\ln\left(1 + b^2 r^2\right)\hat{z}, \quad (8)$$

the relative helicity turns out to be

$$\frac{H_r}{L} = \frac{\pi B_0^2}{2b^3}\left[\ln\left(1 + b^2 R^2\right)\right]^2 = \left(\frac{8\pi[\ln(1 + U^2/4)]^2}{U^4}\right) B_0^2 R^4 \tau_0, \quad (9)$$

where $U = 2\tau_0 R$ as in the previous model.

3.3. Constant Current Field

[16] A nonforce-free model has been recently proposed by *Hidalgo et al.* [2000] and *Hidalgo et al.* [2002] to describe interplanetary structures. This model assumes a constant current density such as $\vec{\mathbf{j}}(\vec{\mathbf{r}}) = j_\varphi\hat{\varphi} + j_z\hat{z}$, where j_φ and j_z are constants. Thus the magnetic field of this configuration is obtained as

$$\vec{\mathbf{B}} = B_0\tau_0 r\hat{\varphi} + B_0(1 - r/R)\hat{z}, \quad (10)$$

where $B_0 = \mu_0 j_\varphi R$ is the maximum field at the center of the tube, and $\tau_0 = j_z/(2j_\varphi R)$ measures the twist at the flux tube axis. The magnetic field lines twist per unit length, is:

$$\tau(r) = \frac{j_z}{2j_\varphi(R - r)} = \frac{\tau_0}{1 - r/R}. \quad (11)$$

The two physical parameters fitted are j_φ and j_z, but for comparison with other models we rather give the corresponding τ_0 and B_0 values.

[17] Next, from equation (2) and

$$\vec{\mathbf{A}} = \frac{B_0 r}{R}(R/2 - r/3)\hat{\varphi} - \frac{B_0}{2}\tau_0 r^2\hat{z}, \quad (12)$$

the relative helicity results,

$$H_r/L = \frac{7\pi\mu_0^2}{60} j_\varphi j_z R^5 = \frac{7\pi}{30} B_0^2 R^4 \tau_0. \quad (13)$$

4. Results

4.1. Data and Method Used

[18] We apply the analytical results derived in the previous section to the hot tube observed by Wind from 24 October 1995, 2100 UT to 25 October 1995, 0600 UT. The 1.5 min resolution magnetic data have been downloaded from the public site http://cdaweb.gsfc.nasa.gov/cdaweb/istp-public/. In order to remove small-scale phenomena (e.g., waves) [*Farrugia et al.*, 1998; *Dasso et al.*, 2003b] and because we are interested only in large-scale field changes, we smoothed the dataset and we present results for ~5 min averaged data, such that the whole event includes 100 points. We obtain comparable results using the original data directly (see at the end of section 4.4).

[19] We first determine the orientation of the flux tube from a minimum variance (MV) analysis of the magnetic observations [*Sonnerup and Cahill*, 1967]. The method finds the direction ($\hat{\mathbf{n}}$) in which the mean quadratic deviation of the field, $\langle(\mathbf{B}\cdot\hat{\mathbf{n}} - \langle\,\mathbf{B}\cdot\hat{\mathbf{n}}\rangle)^2\rangle$, is minimum (maximum). It is possible to show that this is equivalent to find the eigenvector corresponding to the smallest (highest) eigenvalue of the covariance matrix $M_{i,j} = \langle B_i B_j\rangle - \langle B_i\rangle\langle B_j\rangle$. When the minimum distance from the spacecraft to the axis of the flux tube is close to zero, and assuming a nearly cylindrical flux tube, the largest (smallest) change of $\mathbf{B}$ comes from its B_φ (B_r) component. Thus this MV method determines the direction of the maximum ($\hat{\varphi}$), intermediate ($\hat{z}$), and minimum ($\hat{r}$) variance of the field. A more complete discussion of this method applied to interplanetary flux tubes is given in the appendix of *Bothmer* and Schwenn [1998].

[20] In our event, we find a well-defined direction for the principal axis of the tube (corresponding to the intermediate

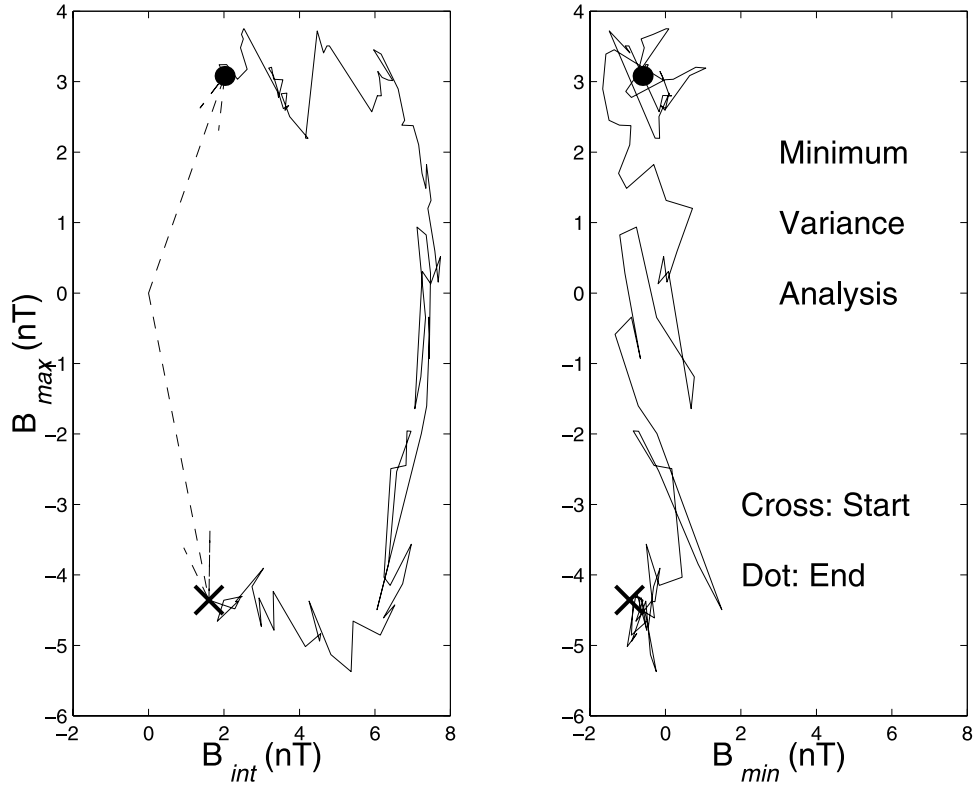

Figure 1. The rotation of the tip of the magnetic field vector in the $B_{max} - B_{int}$ plane (left) as time proceeds. In the $B_{max} - B_{min}$ plane very low fluctuations of B_{min} are evident (right). B_{max}, B_{int}, and B_{min} correspond to B_φ, B_z, and B_r, respectively.

eigenvector) with an intermediate to minimum eigenvalues ratio of ∼11 (so that the field has clearly a different behavior in both directions). Then, with the MV method we define the orientation of the flux tube as defined by the angle (θ) between the ecliptic plane and the axis of the tube, such that when θ = +90° the magnetic field along this axis is aligned with the z unit vector of the GSE (Geocentric Solar Ecliptic) coordinates, and the angle (ϕ) between the direction of the y unit vector of GSE and the projection of the flux-tube axis on the ecliptic plane, measured counterclockwise.

[21] In this approach, the spacecraft impact parameter, p, is not determined and we set it equal to zero, noting that the large angle rotation of the field (∼127°, see Figure 1) indicates that p/R should be small. Then, the MV coordinates have been used to obtain the two physical parameters (τ_0, B_0) that best fit the observations for the three models given in section 3.

[22] Furthermore, to test the validity of the MV method and to determine the impact parameter, we have simultaneously fitted (SF) the tube orientation, p, and the two physical parameters (for each model) using the observed field in GSE (as described by *Hidalgo et al.* [2002]). The least-square fitting has been done in all cases using the standard Levenberg-Marquardt routine [*Press et al.*, 1992].

4.2. Comparison of the Fitting Quality

[23] Figures 2–4 depict the three GSE components of the measured magnetic field, together with the curves obtained from each model. From Figures 2–4 and the values of $\sqrt{\chi^2}$ (see Table 1), we find, as expected, that when a simultaneous fitting (SF) is done a slightly better quality fit than with the MV method is obtained for all three models. The linear force-free field (L) and the uniform twist (G) models fit the observations equally well (with only ∼1% difference

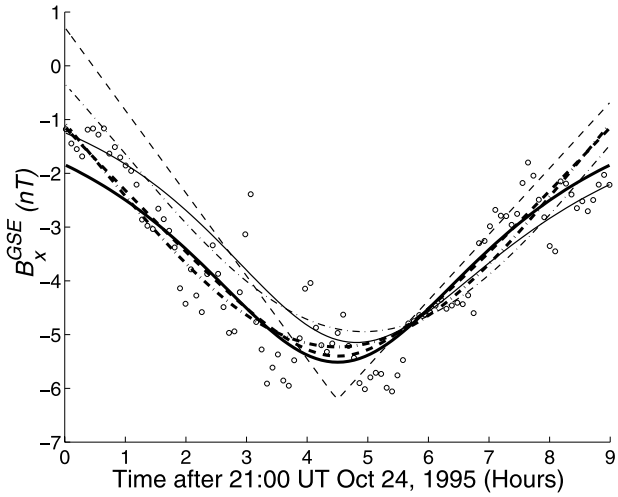

Figure 2. B_x^{GSE} component of the magnetic field (in Geocentric Solar Ecliptic coordinates) for the flux tube observed on 24–25 October 1995. Circles correspond to the observed field (with 5 min averaging), dash-dotted line to the Lundquist model, solid line to the Gold-Hoyle model, and dashed line to the constant current model. Thin and thick lines correspond to a minimum variance (MV) and a simultaneous fit (SF), respectively.

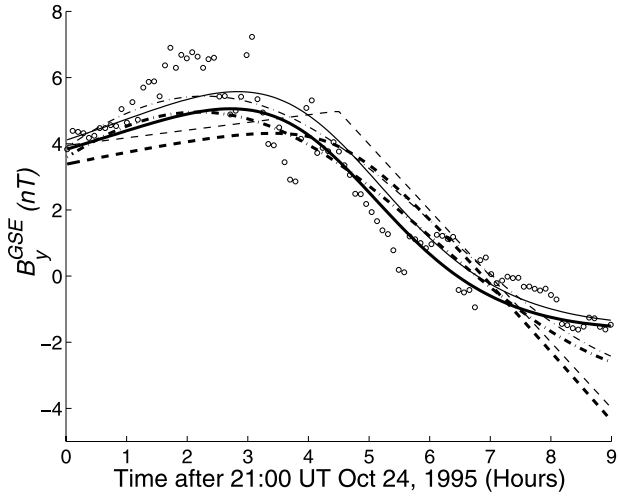

Figure 3. Same as Figure 2 but for B_y^{GSE}.

in the value of $\sqrt{\chi^2}$). So, we cannot discriminate between the two force free models despite the fact that their twist distribution is very different (larger at the border of the flux tube for model L, compared to a uniform distribution for model G, see equations (4) and (7)).

[24] However, according to the $\sqrt{\chi^2}$ value obtained for the constant current model (H), which is larger by ~30–35% with both methods (MV and SF), the model H is significantly farther from the observations than both force-free models. It is worth noting that in the case of model H, a triangular profile is present for the magnetic field computed along any linear orbit that crosses the center of the tube (i.e., zero impact parameter). This direct consequence of the model is reflected in Figures 2–4. However, it is premature to conclude from this local feature, and from our results in a particular case, that model H is less representative of the observations of interplanetary flux tubes than some other model.

4.3. Analysis of the Results

[25] The orientation of the tube with the MV method is such that $\theta \sim -30°$ and $\phi \sim 51°$. θ is modified by ~4° and ϕ by ~1° when the SF method is used with the best quality models (the two force-free models, see Table 1). A much larger change (~8–10°) is present with model H. This important change in the orientation has consequences in the values of all fitted parameters (see Table 1).

[26] With the SF method, the flux tube radius changes at most by 3% compared to its value deduced with the MV method (excluding the H-SF case). The impact parameter is only 8% of R with both force-free models. This result justifies, a posteriori, setting p to zero in the MV method.

[27] The twist, τ_0, per unit length at the tube center is found to be in the range ~20–40 AU^{-1} showing that the flux tube is significantly twisted along its length (with a typical length of ~1 AU, the central part has between 3 and 6 turns). Comparing the MV and SF methods, we find only ~1% difference on τ_0 for a given force-free model. However, it is worth remembering that the twist distribution in the flux tube is strongly model dependent (compare equations (4), (7), and (11)). This implies that the obtained values for τ_0, a local quantity, are not directly comparable between different models; a pertinent comparison can only be done with a global quantity, such as the magnetic helicity (see next section). It follows that it is logical that τ_0 is higher in model G, where the twist is uniformly distributed, while in the two other cases, it is concentrated at the periphery of the flux tube.

[28] The central field strength, B_0, is also well determined; the results are very close with the MV and SF methods and we find only 4% difference between the two force-free models (see Table 1). The field strength B_0 lies in the interval 7.3–7.6 nT, around 6 times the mean variation obtained when the data and the fitted models are compared ($\sqrt{\chi^2} \sim 1.3$ nT). The largest variations, ~20%–40%, are obtained for model H with both methods.

4.4. Magnetic Flux and Helicity

[29] From the fitted model parameters, we can derive global physical quantities. One is the magnetic flux, F, of B_z (i.e., across a section of the flux tube orthogonal to $\hat{z}$). The flux has a narrow range of values in the force-free cases (ninth column in Table 1), $F \sim (1.3–1.4) \times 10^{-2}$ nT AU^2, but it changes by ~±20% for model H in both MV and SF methods.

[30] Another global quantity of interest is the relative magnetic helicity H_r. The observations provide data only along one direction of the MC; however, assuming a cylindrical model, we can derive global quantities per unit length and per unit volume. In the two final columns in Table 1 we show H_r results per unit length (equations (5), (9), and (13)) and divided by the tube volume ($V = \pi R^2 L$). The magnetic field of the flux tube is right-handed so H_r is positive.

[31] In the force-free cases, H_r/L agrees within ±10% and H_r/V within ±5% around their mean values, considering both methods. With the constant current model, the differences found in the obtained parameters (B_0, τ_0, and R) are amplified in the helicity results (since H_r has a nonlinear dependence on these parameters, see equation (13)). The difference in H_r/L with the force-free values can be up to 60%, while it stays below 20% for H_r/V. However, as the fit

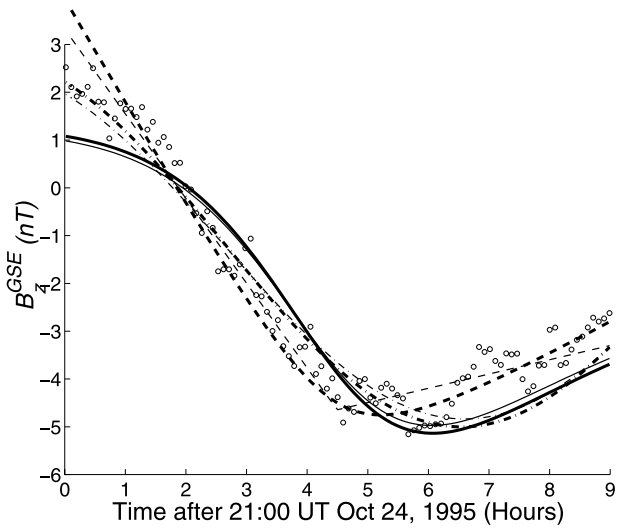

Figure 4. Same as Figure 2 but for B_z^{GSE}.

Table 1. Geometric and Physical Parameters Fitted for the Hot Flux Tube[a]

Model-Method	θ, deg	ϕ, deg	R, 10^{-2}AU	p/R	τ_0, AU^{-1}	B_0, nT	$\sqrt{\chi^2}$, nT	F, 10^{-2}nT AU^2	H_r/L, 10^{-3}nT^{2}AU^3	H_r/V, 10^{-1}nT^{2}AU
L-MV	−30.3	51.2	3.2	0	32.4	7.3	1.35	1.3	1.3	4.2
G-MV	−30.3	51.2	3.2	0	43.8	7.6	1.36	1.3	1.2	3.9
H-MV	−30.3	51.2	3.2	0	17.7	9.2	1.82	1.0	1.1	3.6
L-SF	−34.1	52.6	3.2	0.08	32.0	7.3	1.31	1.3	1.4	4.3
G-SF	−34.6	52.0	3.3	0.08	43.2	7.6	1.33	1.4	1.4	4.1
H-SF	−39.6	44.0	3.8	0.26	13.2	10.7	1.70	1.6	2.2	5.0

[a]The first three rows show the results for the orientation given by the minimum variance (MV) method, while the last three correspond to a simultaneous fit (SF), where both the geometrical and physical parameters are fitted to the data. L, G, and H refer to the Lundquist, Gold Hoyle, and Hidalgo et al. models, respectively. The geometrical parameters are the angle (θ) between the ecliptic plane and the axis of the tube, the angle (ϕ) between the direction of the y unit vector of GSE and the projection of the flux-tube axis on the ecliptic plane (see text), the flux tube radius (R), and the impact parameter (p) measured in units of R. The two physical parameters of the models are the twist per unit length (τ_0) and the intensity of the field (B_0), both at the center of the tube. The quality of the fit is given by the square root of χ^2. Finally, we give the estimated magnetic flux (F), see section 4.4, and the magnetic helicity per unit length (H_r/L) and per unit volume (H_r/V).

is significantly less good with model H, we will only consider the force-free results.

[32] When the full (1.5 min) resolution data are used, we find that θ, ϕ, R, τ_0, B_0, χ^2, and H_r/V differ by less than ∼4%; while F, p, and H_r/L in less than ∼10%, except p in model G for the simultaneous fit, which gives $p/R = 0.05$. So, as expected, the small-scale features have a small effect on the derived global values.

5. Conclusion

[33] Transient solar ejecta have their origin in an instability of the solar coronal field. The magnetic field ejected from the Sun is, theoretically, expected to carry the magnetic helicity of the original solar source and to appear as an interplanetary twisted magnetic flux tube. In order to quantify this link and to better determine the physical characteristics of the solar source region, global quantities, such as the magnetic flux and helicity, are needed. The determined magnetic flux can be compared with the magnetic flux of the coronal region where evidences of field expansion are seen (such as the presence of transient coronal holes). The magnetic helicity is also a useful quantity, because it is conserved and because techniques to measure both coronal values and photospheric fluxes are presently being developed [see, e.g., *Chae*, 2001; *Moon et al.*, 2002; *Nindos and Zhang*, 2002; *Démoulin et al.*, 2002; *Green et al.*, 2002].

[34] We analyzed one example of solar ejecta, quantifying the physical quantities in the interplanetary flux tube observed by Wind on 24–25 October 1995. The measured magnetic field components of the structure have been fitted using two different methods, minimum variance (MV) and simultaneous fitting (SF), and three different models: a linear force-free field (L), a uniformly twisted (G), and a constant current field (H). For this particular flux tube, we find that both force-free models give a significantly better fit to the observations than the constant current model. However, we presently do not know if this is a general characteristic of interplanetary flux tubes and the present analysis needs to be applied to more cases.

[35] Considering only the force-free cases, we find a very close agreement between the results for the MV and SF methods. For example, the flux tube orientation is determined within a 4° range, the radius R with 3% difference, and the field strength B_0, with only 4% difference (see Table 1 and section 4.3).

[36] Despite important variations in the distribution of the twist assumed by the two force-free models, we are unable to select between them. The twist per unit length around the central part of the flux tube differs by ∼25%, when a given method is taken. Indeed, it is more relevant to compare the twist value averaged on the flux tube cross section, such as given by the magnetic helicity. We find only a ±10% variation around the mean in the derived helicity per unit length (H_r/L), and ±5% when it is taken per unit volume (H_r/V), considering both methods. Another well determined global quantity is the magnetic flux, F (defined in section 4.4), we find a ±8% variation around the mean value in this case.

[37] The case studied here is an example. Our next step is to extend our analysis to a large set of interplanetary manifestations of solar ejecta, in particular MCs.

[38] **Acknowledgments.** This research has made use of NASA's Space Physics Data Facility (SPDF). This work was partially supported by the Argentinean UBA grants UBACyT X209 and UBACYT X059, NASA Living with a Star grant NAG5-10883, and NASA grant NAG5-11803. S.D. is a fellow of CONICET and C.H.M. is a member of the Carrera del Investigador Científico, CONICET. C.H.M. and P.D. thank ECOS (France) and SECyT (Argentina) for their cooperative science program A01U04. The authors are grateful to the referees, whose constructive criticisms helped us to improve this paper.

[39] Shadia Rifai Habbal thanks Vasyl Yurchyshyn and another referee for their assistance in evaluating this paper.

References

Berger, M. A., Rigorous new limits on magnetic helicity dissipation in the solar corona, *Geophys. Astrophys. Fluid Dyn.*, *30*, 79–104, 1984.

Berger, M. A., and G. B. Field, The topological properties of magnetic helicity, *J. Fluid. Mech.*, *147*, 133–148, 1984.

Bothmer, V., and R. Schwenn, Eruptive prominences as sources of magnetic clouds in the solar wind, *Space Sci. Rev.*, *70*, 215–220, 1994.

Bothmer, V., and R. Schwenn, The structure and origin of magnetic clouds in the solar wind, *Ann. Geophys.*, *16*, 1–24, 1998.

Burlaga, L. F., Magnetic clouds and force-free fields with constant alpha, *J. Geophys. Res.*, *93*, 7217–7224, 1988.

Burlaga, L. F., *Interplanetary Magnetohydrodynamics*, Oxford Univ. Press, New York, 1995.

Burlaga, L., E. Sittler, F. Mariani, and R. Schwenn, Magnetic loop behind an interplanetary shock—Voyager, Helios, and IMP 8 observations, *J. Geophys. Res.*, *86*, 6673–6684, 1981.

Chae, J., Observational determination of the rate of magnetic helicity transport through the solar surface via the horizontal motion of field line footpoints, *Astrophys. J.*, *560*, 95–98, 2001.

Cid, C., M. A. Hidalgo, T. Nieves-Chinchilla, J. Sequeiros, and A. F. Viñas, Plasma and magnetic field inside magnetic clouds: A global study, *Sol. Phys.*, *207*, 187–198, 2002.

Démoulin, P., C. H. Mandrini, L. van Driel-Gesztelyi, B. J. Thompson, S. Plunkett, Z. Kovári, G. Aulanier, and A. Young, What is the source of the magnetic helicity shed by CMEs? The long-term helicity budget of AR 7978, *Astron. Astrophys.*, *382*, 650–665, 2002.

Dasso, S., C. J. Farrugia, F. T. Gratton, R. P. Lepping, K. W. Ogilvie, and R. J. Fitzenreiter, Waves in the proton cyclotron frequency range in the CME observed by wind on August 7–8, 1996: Theory and data, *Adv. Space Res.*, *28*, 747–752, 2001.

Dasso, S., C. H. Mandrini, and P. Démoulin, The magnetic helicity of an interplanetary hot flux rope, in *Solar Wind Ten*, edited by M. Velli et al., *AIP Conf. Proc. 679*, 786–789, 2003a.

Dasso, S., F. T. Gratton, and C. J. Farrugia, A parametric study of the influence of ion and electron properties on the excitation of electromagnetic ion cyclotron waves in coronal mass ejections, *J. Geophys. Res.*, *108*(A4), 1149, doi:10.1029/2002JA009558, 2003b.

Farrugia, C. J., V. A. Osherovich, and L. F. Burlaga, Magnetic flux rope versus the spheromak as models for interplanetary magnetic clouds, *J. Geophys. Res.*, *100*, 12,293–12,306, 1995.

Farrugia, C. J., L. F. Burlaga, and R. P. Lepping, Magnetic clouds and the quiet/storm effect at Earth: A review, in *Magnetic Storms*, *Geophys. Monogr. Ser.*, vol. 98, edited by B. T. Tsurutani et al., pp. 91, AGU, Washington, DC, 1997.

Farrugia, C. J., F. T. Gratton, G. Gnavi, and K. W. Ogilvie, On the possible excitation of electromagnetic ion cyclotron waves in solar ejecta, *J. Geophys. Res.*, *103*, 6543–6550, 1998.

Farrugia, C. J., et al., A uniform-twist magnetic flux rope in the solar wind, in *Solar Wind Nine*, edited by S. Habbal et al., *AIP Conf. Proc., 471*, 745–748, 1999.

Fletcher, L., M. C. López Fuentes, C. H. Mandrini, B. Schmieder, P. Démoulin, H. E. Mason, P. R. Young, and N. Nitta, A relationship between transition region brightenings, abundances, and magnetic topology, *Solar Phys.*, *203*, 255–287, 2001.

Glover, A., N. D. R. Ranns, L. K. Harra, and J. L. Culhane, The onset and association of CMEs with sigmoidal active regions, *Geophys. Res. Lett.*, *27*, 2161–2164, 2000.

Gold, T., and F. Hoyle, On the origin of solar flares, *Mon. Not. R. Astron. Soc.*, *120*, 89–105, 1960.

Gonzalez, W. D., B. T. Tsurutani, and A. L. Clúa de Gonzalez, Interplanetary origin of geomagnetic storms, *Space Sci. Rev.*, *88*, 529–562, 1999.

Gosling, J. T., Coronal mass ejections and magnetic flux ropes in interplanetary space, in *Physics of Magnetic Flux Ropes*, *Geophys. Monogr. Ser.*, vol. 58, edited by C. T. Russell, E. R. Priest, and L. C. Lee, pp. 343–364, AGU, Washington, DC, 1990.

Green, L. M., M. C. López Fuentes, C. H. Mandrini, P. Démoulin, L. Van Driel-Gesztelyi, and J. L. Culhane, The magnetic helicity budget of a cme-prolific active region, *Solar Phys.*, *208*, 43–68, 2002.

Hidalgo, M. A., C. Cid, J. Medina, and A. F. Viñas, A new model for the topology of magnetic clouds in the solar wind, *Sol. Phys.*, *194*, 165–174, 2000.

Hidalgo, M. A., C. Cid, J. Medina, A. F. Viñas, and J. Sequeiros, A nonforce free approach to the topology of magnetic clouds in the solar wind, *J. Geophys. Res.*, *107*(A1), 1002, doi:10.1029/2001JA900100, 2002.

Hu, Q., and B. U. Ö. Sonnerup, Reconstruction of magnetic flux ropes in the solar wind, *Geophys. Res. Lett.*, *28*, 467–470, 2001.

Leamon, R. J., R. C. Canfield, and A. A. Pevtsov, Properties of magnetic clouds and geomagnetic storms associated with eruption of coronal sigmoids, *J. Geophys. Res.*, *107*(A9), 1234, doi:10.1029/2001JA000313, 2002.

Lepping, R. P., L. F. Burlaga, and J. A. Jones, Magnetic field structure of interplanetary magnetic clouds at 1 AU, *J. Geophys. Res.*, *95*, 11,957–11,965, 1990.

Lundquist, S., Magnetohydrostatic fields, *Ark. Fys.*, *2*, 361–365, 1950.

Marubashi, K., Interplanetary magnetic flux ropes and solar filaments, in *Coronal Mass Ejection*, *Geophys. Monograph Ser.*, vol. 99, edited by N. Crooker, J. Joselyn, and J. Feynman, pp. 147–156, AGU, Washington, DC, 1997.

Matthaeus, W. H., Magnetic helicity and homogeneous turbulence models, in *Magnetic Helicity in Space and Laboratory Plasmas*, *Geophys. Monogr. Ser.*, vol. 111, edited by M. R. Brown, R. C. Canfield, and A. A. Pevtsov, pp. 247–255, Washington, DC, 2000.

Moon, Y.-J., J. Chae, H. Wang, G. S. Choe, and Y. D. Park, Impulsive variations of the magnetic helicity change rate associated with eruptive flares, *Astrophys. J.*, *580*, 528–537, 2002.

Mulligan, T., and C. T. Russell, Multispacecraft modeling of the flux rope structure of interplanetary coronal mass ejections: Cylindrically symmetric versus nonsymmetric topologies, *J. Geophys. Res.*, *106*, 10,581–10,596, 2001.

Nindos, A., and H. Zhang, Photospheric motions and coronal mass ejection productivity, *Astrophys. J.*, *573*, L133–L136, 2002.

Osherovich, V. A., C. J. Farrugia, L. F. Burlaga, R. P. Lepping, J. Fainberg, and R. G. Stone, Polytropic relationship in interplanetary magnetic clouds, *J. Geophys. Res.*, *98*, 15,331–15,342, 1993.

Press, W. H., S. A. Teukolsky, W. T. Vetterling, and B. P. Flannery, *Numerical Recipes*, Cambridge Univ. Press, New York, 1992.

Richardson, I. G., and H. V. Cane, Regions of abnormally low proton temperature in the solar wind (1965–1991) and their association with ejecta, *J. Geophys. Res.*, *100*, 23,397–23,412, 1995.

Richardson, I. G., C. J. Farrugia, and H. V. Cane, A statistical study of the behavior of the electron temperature in ejecta, *J. Geophys. Res.*, *102*, 4691–4700, 1997.

Rust, D. M., Spawning and shedding helical magnetic fields in the solar atmosphere, *Geophys. Res. Lett.*, *21*, 241–244, 1994.

Smith, C. W., Solar-cycle, radial and longitudinal variations of magnetic helicity: IMF observations, in *Magnetic Helicity in Space and Laboratory Plasmas*, *Geophys. Monogr. Ser.*, vol. 111, M. R. Brown, R. C. Canfield, and A. A. Pevtsov, pp. 239–245, AGU, Washington, DC, 2000.

Sonnerup, B. U., and L. J. Cahill, Magnetosphere structure and attitude from Explorer 12 observations, *J. Geophys. Res.*, *72*, 171–183, 1967.

Yurchyshyn, V. B., H. Wang, P. R. Goode, and Y. Deng, Orientation of the magnetic fields in interplanetary flux ropes and solar filaments, *Astrophys. J.*, *563*, 381–388, 2001.

S. Dasso and C. Mandrini, Instituto de Astronomía y Física del Espacio (IAFE), CC 67 Suc. 28, 1428 Buenos Aires, Argentina. (dasso@df.uba.ar; mandrini@iafe.uba.ar)

P. Démoulin, Observatoire de Paris, section Meudon, LESIA, Bat. 14, F-92195 Meudon Principal Cedex, France. (pascal.demoulin@obspm.fr)

C. J. Farrugia, Institute for the Study of Earth, Oceans, and Space, University of New Hampshire, Durham, NH 03824, USA. (charlie.farrugia.unh.edu)